A Compact Snap-shot Range-Imaging Receiver

Bedabrata Pain, Larry Matthies, Bruce Hancock, and Chao Sun
Jet Propulsion Laboratory
California Institute of Technology
4800 Oak Grove Drive, Pasadena, CA 91109
Phone: 818-354-8765; Fax: 818-393-0045; Email: bpain@jpl.nasa.gov

Range imaging is of great interest for a number of robotic, machine-vision and computer-vision applications. Military vision systems are also expected to largely rely on range imaging for target identification, recognition, and tracking applications. Range imaging is typically carried with the LIDAR technique. The main concept of range measurement using LIDAR is to send out a light pulse from a source, and measure the roundtrip time of flight for the light pulse to travel from the source, get reflected back from a target, and get detected at the detector [1]. Direct measurement of time of flight imposes severe requirements on the detector. For instance, 1 cm range accuracy requires time measurement with better than 30 psec resolution. As a result, LIDARs typically use single well-calibrated detectors and mechanical scanning to build up the range map of a scene. Recently, there has been some progress in using small format Geiger mode avalanche photodiode (APD) detector arrays to provide 3-dimensional LIDAR imaging.

Another successful technique involves stereo-vision that determines distance by triangulation of features on the object plane by using two or more cameras [2]. The disadvantages of stereo-vision include the need for multiple cameras with adequate separation (baseline), the need for significant processing resources, and inoperability in scenes with low contrast or texture. Other range finding techniques such as range extraction from variable focus images, image motion or image shape often suffer from the need for unwarranted apriori assumptions about the object shape, multiple iterations, and high frame rate requirements.

Our technique of range mapping involves an indirect time-of-flight measurement by calculating the phase delay. The main benefit of this approach is that the GHz clocking needed in LIDAR systems is replaced by a much lower frequency (~ 20 MHz) modulation, resulting in a solid-state array-based implementation of range detectors. In turn, this allows the implementation of a staring imager system that provides an instantaneous (snapshot) range map of the scene or 3D imaging.

Figure 1 shows the concept of the flash LADAR. It is an active system – consisting of a source and a receiver (detector) pair. The laser source (pulsed or continuous) is coupled to a diffuser to illuminate the scene field-of-view (FOV) of interest. The reflected laser pulse is focused by the imaging optics on the receiver (detector) pixels. Range-to-target is measured by detecting and computing the phase of the return pulse with respect to an electronic local oscillator (LO) in each pixel. Since the phase delay is proportional to the time-of-flight, each pixel generates a signal that is proportional to the range of target imaged by the pixel.

While the phase detection approach has been used in other range imaging systems, our measurement approach is different from the published methods [3,4,5]. In our method, each pixel consists of a detector coupled to multiple phase-to-voltage converters. A phase-to-voltage converter is implemented as a multiplier or a mixer, where the instantaenous LO voltage is multiplied by the detected photocurrent.

The pixel front-end consists of a photodiode that converts the optical laser pulse to a photocurrent pulse. The photocurrent is mirrored by the source-modulated current mirror pair. Unlike a conventional current mirror, the source of the mirror-FET is modulated by a synchronized electronic local oscillator (LO) excitation. The output drain current of the mirror FET is:

$$I_{drain} = \alpha \cdot I_{pulse}(t - t_d) \cdot \exp(V_s) = \alpha \cdot I_{pulse}(t - t_d) \cdot \exp(V_o \sin(2\pi f_c t))$$
$$\approx \alpha \cdot I_{pulse} \cdot \exp(V_o \sin(2\pi f_c t_d)) \approx \alpha \cdot I_{pulse} \cdot [1 + V_o \sin(2\pi f_c t_d)]$$

where α is a proportionality factor of current-mirroring, I_{pulse} is the magnitude of the photocurrent pulse, t_d is the delay of the laser pulse return with respect to LO, V_o and f_c are the amplitude and the frequency of the LO carrier frequency respectively. The source-modulated current mirror generates an output drain current that is proportional instantaneous value of the LO sinewave at the point of laser pulse return (t_d). If the photocurrent pulse is broad (e.g ~ 20-40 ns) with respect to the LO frequency, then I_{drain} is proportional to

the integral of the sinewave, instead of the instantaenous value. The drain current is integrated on a capacitor to generate a low-noise voltage corresponding to the phase. Thus, each source-modulated current-mirror operates as a phase-to-voltage converter or a phase-detector.

Figure 2 shows the detailed circuit in each pixel. In order to detect signals with current pulses as narrow as ~ 20-40 nsec duration, the front-end bandwidth needs to be increased. This has been achieved by using a negative feedback amplifier with gain ~ 60 dB to provide the necessary speed improvement. The feedback holds the photodiode potential fixed, improving the response time by a factor equal to the gain of the opamp, enabling detection of pulses of duration as small as 10 nsec.

Range measurement in a typical scene also has to contend with background illumination and target albedo, both of which will cause a change in the output voltage. Each pixel consists of 4 phase-detectors: first three being simultaneously excited by 120° phase delayed sinewaves to eliminate ambiguities caused by the background illumination and target albedo; and the fourth one excited by a lower frequency (10-50x lower) sinewave for resolving phase ambiguities due to 2π periodicity. The first three outputs can be differentially combined to compute the range independent of background illumination and target albedo. The detected range (R) is: $R = \frac{c}{4\pi f_c} \tan^{-1}\left[\frac{(m_1 - m_2) + (m_1 - m_3)}{\sqrt{3}(m_2 - m_3)}\right]$ where m_i are the output from 3 phase-detectors in each pixel. The differential measurement also provides immunity of common-mode noise and front-end noise.

We have developed a proof-of-concept 128x1 pixel array to determine the feasibility of the technique. The array consists of pixels in 50 μm pitch, and four phase-detectors per pixel. Figure 3 shows the picture of the chip, and the layout of the pixel.

Figure 4 shows the demonstration of phase detection operation. The measurement was carried out as follows. The output of one pixel was measured by fixing a target, and by changing the delay between triggering of the laser pulse and the local oscillator in 2.5 nsec increments. Figure 4 shows that the phase-detector faithfully reproduced the phase of the local oscillator (frequency 10 MHz), even though the input pulse duration was as much as 40 nsec.

Proof-of-concept range measurement was carried out by reflecting the laser pulse from a fixed wall and moving the detector platform towards it. Figure 5 shows the measured range as a function of the distance of the detector platform from the fixed wall. It shows that detector circuit is capable of resolving range as small as 1 cm over a range depth of > 5 meters. Response non-uniformity was measured by looking for the spatial variance of the data from the 128 channels and using a flat target. Due to the inherent gain and offset variations within the in-pixel multipliers as well as due to routing delays in distributing the LO across the array, off-chip gain and offset calibration was required. Figure 6 shows the range resolution error from one pixel to another. After calibration, the residual non-uniformity error is less than 2% across the array, except towards the edge. No inter-channel modulation (i.e. between the phase detectors in each pixel) was observed, and the on-chip distribution of LO is uniform enough that no gradient in range detection is observed. The minimum photo-detection limit corresponds to ~ 200 electrons per photocurrent pulse. Table 1 summarizes the performance results of the range-imaging array.

Acknowledgments:

This research was carried out at the Jet Propulsion Laboratory, California Institute of Technology, under a contract with the National Aeronautics and Space Administration.

References:

1. M.D. Adams, *IEEE Sensors Journal*, vol. 2(1), pp. 2-13, 2002.
2. S.T. Barnard et al., *IEEE Trans. Pattern Anal. Mach. Intell*, vol. 2(4), pp. 333-340, 1980.
3. R. Lange et al., *IEEE J. Quantum Electron.*, vol. 37, pp. 390–397, 2001.
4. O. Elkhalili et al., *IEEE J. Solid-state Circuits*, vol. 39, no. 7, 2004, pp. 1208-1212
5. S. Burak Gokturk et al., *Proc. 2004 IEEE Computer Society Conference on Computer Vision and Pattern Recognition Workshops (CVPRW'04).*

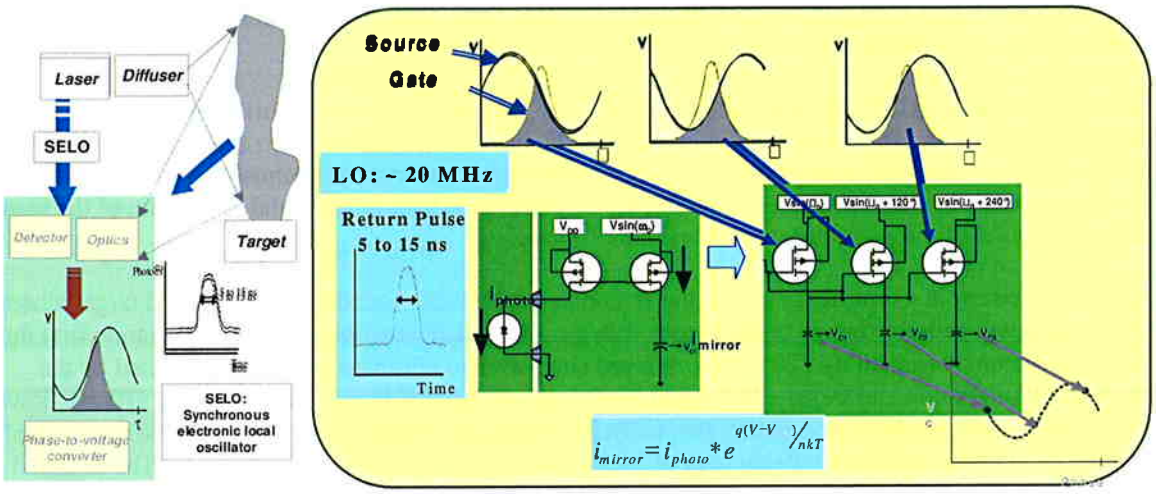

Figure 1: Range imaging concept: Active flash LADAR system (left), and phase-detection concept (right)

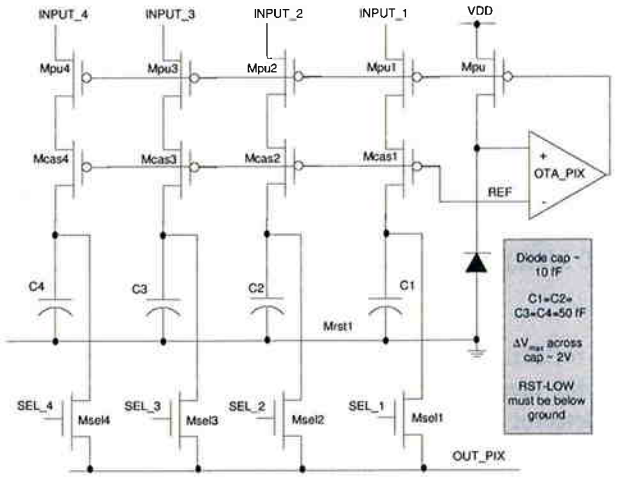

Figure 2: Detailed circuit diagram of each pixel

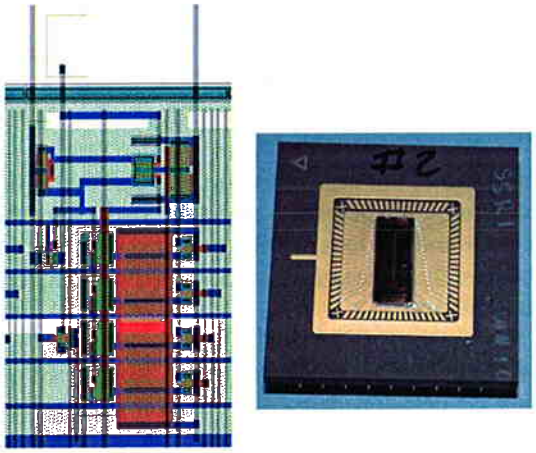

Figure 3: Pixel layout (left) and picture of the detector-chip (right)

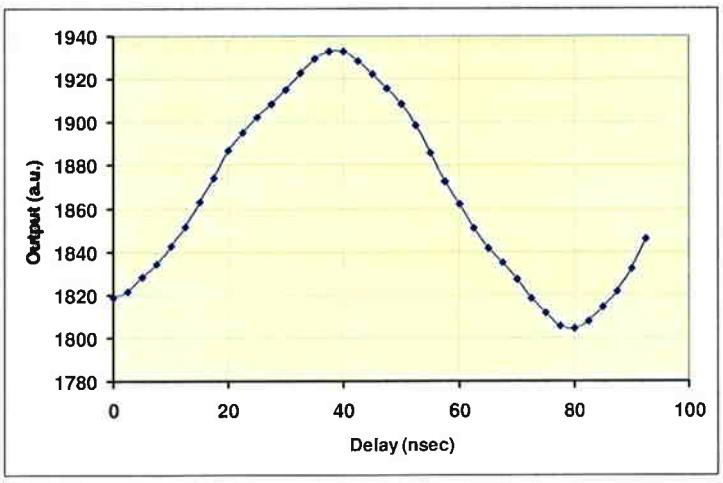

Figure 4: Proof of concept phase detection with a40 ns laser pulse – the LO is reconstructed from the phase samples collected by each pixel

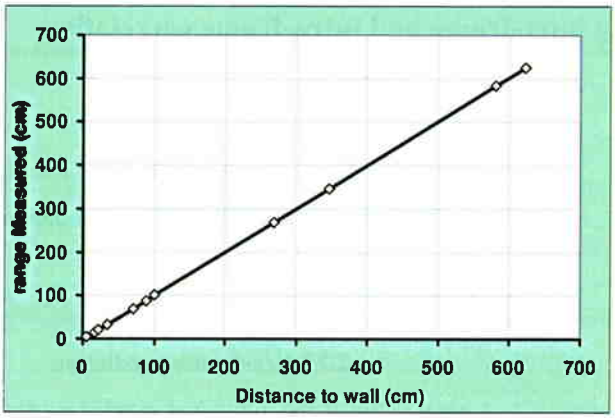

Figure 5: Measured range vs distance between target and the detector platform

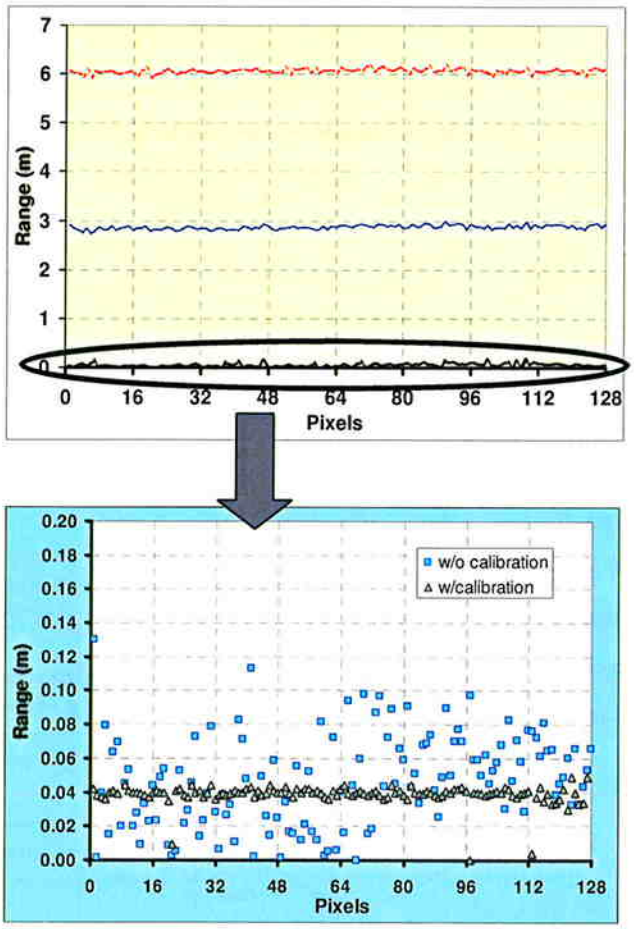

Figure 6: Range measurement uniformity for the 128x1 array: graph on the right shows a blow up of the smallest range detected

Table 1: Performance characteristics of the proof-of-concept detector array

Parameters	Values
Array Size	128x1
Pixel Pitch	50 μm
# of mixers/pixel	4
LO frequency	20 MHz; 1 MHz
Wavelength	830 nm
Return Pulse width	40 nsec
Min. detected current	0.85 nA
Min. detected electrons	210 e^-
Quantum efficiency	>20%
Min. detected range	< 2 cm
Range depth	> 7 m
Range non-uniformity	< 2%
Repetition rate	> 100 Hz
Power dissipation	< 30 mW